Long-Chain Branching in Metallocene-Catalyzed Polyethylenes Investigated by Low Oscillatory Shear and Uniaxial Extensional Rheometry

Anneli Malmberg,[†,§] Claus Gabriel,[‡] Thomas Steffl,[‡] Helmut Münstedt,[‡] and Barbro Löfgren*[,†]

Polymer Science Centre, Helsinki University of Technology, P.O. Box 356, FIN-02151 Espoo, Finland, and Institute of Polymer Materials, University of Erlangen-Nürnberg, Martensstrasse 7, D-91058 Erlangen, Germany

Received May 1, 2001; Revised Manuscript Received September 4, 2001

ABSTRACT: This paper explores shear and extensional rheological behavior of unimodal, metallocene-catalyzed polyethylenes with low contents of long-chain branching (LCB). The polymers were produced in semibatch slurry polymerizations with methylaluminoxane (MAO) activated metallocene catalysts bis(*n*-butylcyclopentadienyl)hafnium dichloride (**1**), *rac*-[ethylenebis(2-*tert*-butyldimethylsiloxy)indenyl)]-zirconium dichloride (**2**), *rac*-[ethylenebis(1-*tert*-butyldimethylsiloxy)indenyl)]zirconium dichloride (**3**), and *rac*-[ethylenebis(1-triisopropylsiloxy)indenyl)]zirconium dichloride (**4**). Melt properties in low oscillatory shear, in contrast to molecular weight and molecular weight distribution data from gel permeation chromatography, suggested that the polymers prepared with the ethylene-bridged complexes **2**, **3**, and **4** contain small but different amounts of LCB. In the melt uniaxial elongation experiments, the long-chain branched polymers exhibited strain hardening at all extension rates (rate range was from 1.0 to 0.01 s^{-1}) with continual increase in strain hardening toward low strain rates. Unexpectedly, the behavior in LVE regime low shear and uniaxial elongation in the nonlinear range arranged the polymers in dissimilar order of apparently increasing LCB. Even though both these rheological techniques are sensitive to the molecular structure, they evidently reveal different features of it. Variation in the distribution (topology) of the long-chain branching due to differences in catalyst systems offers a plausible explanation of the differences in uniaxial elongation.

Introduction

Since the announcement of the ability of the Dow constrained-geometry catalyst (CGC) to produce small amounts of long-chain branching (LCB),[1,2] it has repeatedly been reported that also conventional bis(cyclopentadienyl)-based metallocene complexes have the ability to produce low levels of long-chain branching.[3−8] Although other mechanisms have been put forward,[9] it is fairly well accepted that the mechanism of LCB formation in both CGC and conventional metallocene-catalyzed polymerizations is copolymerization of vinyl-terminated polyethylene molecules. The first requirement in producing long-chain branching via copolymerization is the presence of termination mechanisms producing vinyl-terminated macromonomers. Second, the catalyst must be able to incorporate these macromonomers into a growing chain. In accordance with the copolymerization mechanism, the rheological behavior of metallocene-catalyzed ethylene homopolymers has been found to heavily depend on the polymerization conditions: ethylene pressure, hydrogen concentration, and polymerization time.[7,8,10]

Bearing in mind the mechanism of LCB formation by copolymerization, it can be argued, however, that catalyst structure should still govern the facility of the process. The dominating termination reaction and sensitivity to the presence of chain transfer agents[7,11] are determined by the catalyst. Provided that vinyl ends are formed, even more important aspect may then be copolymerization ability.[8,11−13] In general, the more rigid bridged catalysts copolymerize short-chain α-olefins fairly easily, and they also appear to produce long-chain branching more easily than unbridged metallocenes.[7,8] Another structural feature of the catalyst, besides the bridging, is the size and position of substituents in the ligands. The copolymerization ability can be influenced by position of large substituents in ligands of the metallocene complex: $Et(Ind)_2ZrCl_2$-based metallocene complexes with large siloxy substituent exhibit different copolymerization ability toward short-chain α-olefins according to whether the substituent is in the 1- or 2-position of the indenyl ligand.[12,13] The primary termination reaction in ethylene polymerization with these catalysts appears to be chain transfer to monomer,[11] leading to relatively large amounts of chains with (polymerizable) vinyl bond at the end. Accordingly, both 1- and 2-siloxy-substituted complexes give polymers with rheological behavior indicative of long-chain branching.[8,11]

Characteristically, the long-chain branching produced with the metallocenes seems to be present in very small amounts, often not detectable by NMR or combined GPC detector techniques[14,15] with the detection limit of 1 branch/10000C. In the low shear rate rheological behavior, low levels of LCB manifest themselves as a zero-shear viscosity η_0 higher than that of corresponding linear polymers of similar M_w, as increased shear sensitivity, and as increased melt elasticity.[4−8,10,11,14−19] Even though the effects of the metallocene-generated LCB go beyond the effect of broadening molecular

† Helsinki University of Technology.
‡ University of Erlangen-Nürnberg.
§ Current address: Borealis Polymers Oy, P.O. Box 330, FIN-06101 Porvoo, Finland.
* Corresponding author.

10.1021/ma010753l CCC: $22.00
Published on Web 12/20/2001

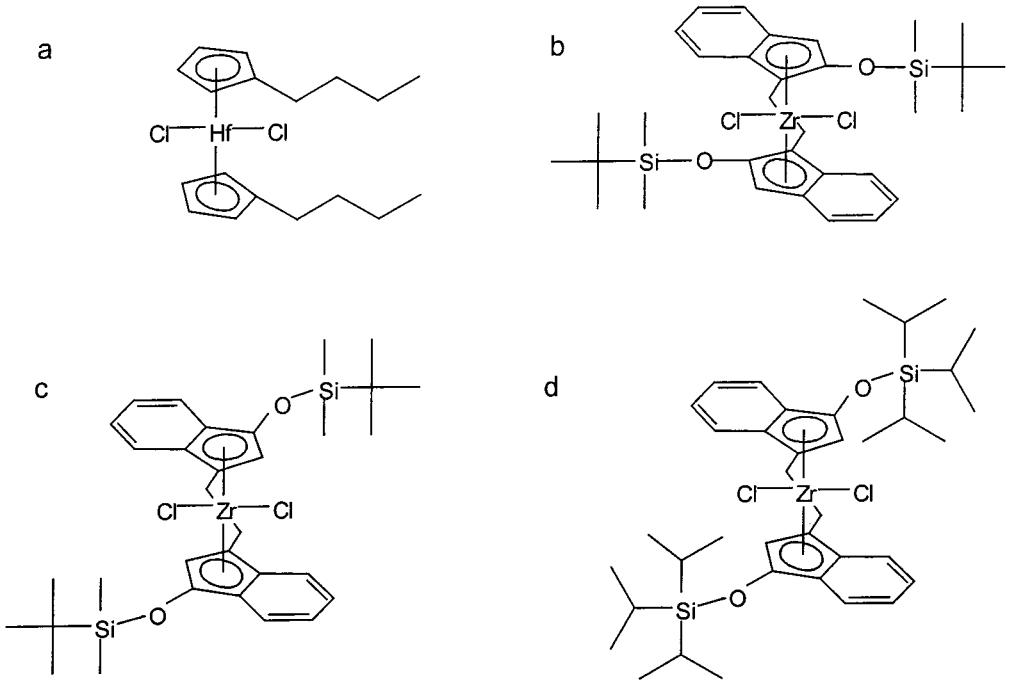

Figure 1. Metallocene structures: (a) bis(*n*-butylcyclopentadienyl)hafnium dichloride (catalyst **1**), (b) *rac*-[ethylenebis(2-*tert*-butyldimethylsiloxy)indenyl)]zirconium dichloride (catalyst **2**), (c) *rac*-[ethylenebis(1-*tert*-butyldimethylsiloxy)indenyl)]zirconium dichloride (catalyst **3**), and (d) *rac*-[ethylenebis(1-tri-isopropylsiloxy)indenyl)]zirconium dichloride (catalyst **4**).

weight distribution (MWD),[20−22] the central problem in the rheological characterization is how to separate the effects of molecular weight, MWD, and LCB.

Another rheological technique sensitive to the presence of LCB is melt uniaxial extensional rheometry.[24−28] The most significant property in this respect is nonlinear behavior in the extensional flow, i.e., strain hardening. Uniaxial extensional rheometry has occasionally been used for the characterization of metallocene-polymerized materials.[21,29,30] These studies have shown strain hardening behavior in materials where the presence of LCB has been demonstrated by NMR and low shear rheological behavior. The conclusions drawn from the findings have been slightly contradictory, however. Wood-Adams et al.[21] concluded that the behavior in uniaxial elongation did not allow materials of different LCB level to be differentiated, whereas Bin Wadud et al.[29] found increasing nonlinearity (strain hardening) with increasing LCB. Chai[30] reported behavior similar to that of LDPE in a broad MWD, long-chain branched polymer catalyzed with a metallocene.

In this study, we explore low oscillatory shear and uniaxial extensional rheological behavior of unimodal, metallocene-catalyzed polyethylenes with low contents of long-chain branching (LCB). An unbridged metallocene complex, *n*-BuCp_2HfCl_2, and three different ethylene-bridged metallocene complexes with a siloxy substituent in either the 1- or 2-position were utilized to produce ethylene/1-hexene copolymers and one ethylene homopolymer. The aim was to vary the level of LCB in the polymers through the choice of the catalyst. Indeed, investigation of the low shear rate rheological behavior by procedures recently outlined in the literature[15,19,22] suggested variation in the degree of LCB from linear to well branched. The melt uniaxial elongation experiments were conducted with a Münstedt-type uniaxial extensional rheometer. Whereas the linear polymer showed no strain hardening at all, the long-chain branched polymers exhibited marked strain hardening character at all extension rates (rate range was from 1.0 to 0.01 s^{-1}). Interestingly enough, the low shear rate properties and the nonlinear behavior in uniaxial elongation ordered the polymers in different ways. The polymer with only moderate changes in low shear rheology showed most pronounced strain hardening, while the polymer with shear properties suggesting highest degree of LCB showed lower degree of strain hardening and different rate dependence of the nonlinear behavior. We propose variation in the LCB topology as a result of the catalyst choice as a plausible explanation for the differences in uniaxial elongation.

Preliminary results of this study have been reported elsewhere.[31]

Methods and Materials

Polymerization and Pelletization. Eight ethylene/hexene copolymers and one ethylene homopolymer were produced in unimodal semibatch slurry polymerizations with various supported metallocene catalysts activated with methylaluminoxane (MAO). The metallocene compound in catalyst **1** was bis(*n*-butylcyclopentadienyl)hafnium dichloride and that in catalyst **2** *rac*-[ethylene bis(2-*tert*-butyldimethylsiloxy)indenyl)]-zirconium dichloride. In catalyst **3** it was *rac*-[ethylenebis(1-*tert*-butyldimethylsiloxy)indenyl)]zirconium dichloride and in catalyst **4** *rac*-[ethylenebis(1-triisopropylsiloxy)indenyl)]zirconium dichloride. The structures of the metallocene complexes are shown in Figure 1. Polymerizations were run in isobutane medium in a 5 L reactor, and hydrogen was used to control the molecular weight. Reactor powders were stabilized with 2000 ppm Irganox B561 before pelletization. Reactor powders were pelletized with a small-scale Brabender compounder−extruder, where the temperature was 230 °C in the barrel and 240 °C at the die, except for polymers C2–P55 and C4–P56, which were extruded at lower temperature (barrel, 180 °C, and die, 190 °C).

Characterization. Apparent molecular weights (M_w and M_n) and molecular weight distribution (MWD) were determined in trichlorobenzene at 135 °C with a Waters high-temperature gel permeation chromatograph (GPC) equipped with refraction index (RI) detector. The GPC was calibrated

Table 1. Sample Characteristics

sample	catalyst	density, g/cm^3	$MFR_{2.16}$, g/10 min	M_w, g/mol	MWD	η_0(190 °C), Pa·s	M_b	α, relative LCB content	$E_{a(aver)}$, kJ/mol
C1_P6	**1**	924	4.6	82 000	3.1	3 130	81 100	9.7×10^{-7}	33
C1_P5	**1**	922	1.5	106 000	3.3	7 970	104 400	1.0×10^{-6}	32
C1_P4	**1**	920	n.d.[b]	169 000	3.9	n.m.	n.m.	n.m.	32
C2_P55	**2**	923	2.4	92 000	3.4	7 260	86 800	4.6×10^{-6}	33
C2_P1	**2**	925	1.5	94 000	3.3	16 600	81 400	1.2×10^{-5}	34
C3_P3	**3**	924	12.0	58 000	4.6	1070	56 000	4.2×10^{-6}	39
C3_P2	**3**	960	5.8	83 000	4.7	10 200	71 400	1.4×10^{-5}	39
C4_P56	**4**	922	12.8	58 000	6.1	1 200	55 300	5.9×10^{-6}	37
C4_P7	**4**	930	1.9	82 000	7.5	25 000	59 700	3.2×10^{-5}	44
LDPE		923	1.9	155 000[a]	15[a]	7 600	n.m.	n.m.	53

[a] Measured with GPC−on-line viscometer, average branching index $g' = 0.5$. [b] n.d. = not determined.

with narrow MWD polystyrene standards covering the molecular weight region from 10^3 to 10^7 g/mol. The calibration curve for polystyrene was converted to linear polyethylene using the Mark−Houwink constants $K = 42 \times 10^5$ and $a = 0.73$. The GPC−on-line viscometer measurements were carried out at 140 °C with use of a Waters 150cvplus instrument equipped with refractometer index and intrinsic viscosity detectors. Double-bond patterns for unstabilized samples were studied with a Nicolet Magna FTIR instrument by the method published by Haslam.[32]

A commercial LDPE manufactured by Borealis served as a reference material in the rheological experiments.

Oscillatory shear rheological measurements in the linear viscoelastic region were run under nitrogen at three temperatures, at 170, 190, and 210 °C on a Rheometric Scientific controlled stress rheometer SR-500. SR-500 was also used for constant stress (creep) measurements, where constant stress was applied on the sample at 190 °C for 1000−1500 s. Two different stress values between 2 and 14 Pa were used for each sample, using a new sample each time. Very low shear rates from 2×10^{-4} to 2×10^{-3} s^{-1} were achieved in these tests, and the viscosity values corresponding to the lowest shear rate achieved are reported as η_0 values. Steady shear start-up tests (shear rate 0.01 s^{-1}, temperature 150 °C) were carried out on an ARES instrument manufactured by Rheometric Scientific. The ARES was also used in studies of thermal stability under air at 150 °C using dynamic time sweeps at frequency of 0.1 rad/s.

Data from the oscillatory shear measurements were utilized to determine the Arrhenius-type flow activation energy, E_a, values according to the relation

$$a_T = \exp\left[\frac{E_a}{R}\left(\frac{1}{T} - \frac{1}{T_0}\right)\right] \quad (1)$$

The shift factor a_T was determined using data of the whole frequency range measured to obtain an average shift factor $a_{T(aver)}$. Data from 190 °C served as the reference. The flow activation energy E_a was calculated from the slope of the linear fit of the shift factors against $1/T$. Correlation factor R2 values greater than 0.99 were achieved in the line fit. The results are displayed in Table 1 as E_a(aver). We concede that the E_a determined this way are not based on η_0 values, and thus they may depend on the range of the oscillatory shear data used for the determination. Nevertheless, the E_a determined in this way fully serves our purpose of classifying the polymers relative to one another.

Characterization by Uniaxial Elongation. The elongation experiments on melts were carried out with a uniaxial extensional rheometer of Münstedt design, which allows experiments to be run in constant strain rate as well as in constant stress mode with high accuracy. The rheometer has recently been described in detail by Kurzbeck et al.[27] and by Münstedt et al.[28] In the rheometer, the sample is stretched vertically in a silicon oil bath, where the density of the oil matches the density of the molten polyethylene.

Sample preparation for the uniaxial elongation experiments started with extrusion through a melt indexer at 150 °C into a mixture of water and ethanol. The cylindrical samples obtained in this way were annealed in a silicon oil bath at 150 °C for 12 min. After this, samples were cut into rods, and both ends of the rod were glued to metal holder clips. Measurements were performed at 150 °C. Constant strain rate experiments were run with several elongation rates: 0.01, 0.03, 0.1, 0.3, 0.5, and 1.0 s^{-1}. Each constant strain rate experiment was done three times, and the results shown represent average of these three measurements. An example of the very small variance in the result of different runs will be displayed in Figure 9. Sample length in the constant strain rate tests was 25 mm, and the maximum length of the sample in the rheometer was 500 mm. Using the Hencky strain measure for strain ϵ

$$\epsilon = \ln \frac{L}{L_0} \quad (2)$$

where L is the sample length fully elongated and L_0 is the original sample length, we obtained maximum strain of 3 in the constant strain rate tests. We also carried out constant stress (creep) experiments with shorter sample length, 10 mm. With this sample length the maximum Hencky strain obtained was 3.9. Following Münstedt et al.,[28] in the constant stress tests the achievement of steady state was determined from plots of the time derivative of strain rate ϵ vs time.

Thermal Stability. As explained above, sample preparation for the extensional rheometer involved additional thermal treatment steps. Considering the sensitivity of extensional rheological behavior to molecular structure, thermal stability of the samples is of extreme importance, especially as measurable contents of double bonds were found in the polymers. The presence of even trace amounts of vinyl-type unsaturation in polymers promotes chain lengthening or branching over chain breakage if stabilization is insufficient[33] and, further, cross-linking reactions due to insufficient stabilization intensify the nonlinear behavior at low extension rates.[34] FTIR study of the reactor powders revealed 0.1 vinyl bonds/1000C in C1_P5, 0.2/1000C in C2_P1, 0.29/1000C in C2_P55, and 0.36/1000C in C4_P56. All polymers were stable during the oscillatory shear tests under nitrogen. For uniaxial elongation tests, the stability is often studied under more severe conditions: in shear without nitrogen blanket at 150 °C. At prolonged times in this more severe test, the polymers showed changes indicative of chain linking reactions. However, during the time required for the extensional sample preparation (1200 s), the change was less than 1% in C1 polymer P5 and less than 3% in C1_P4 (at time 1800 s). The increase in G' with time was highest, 5%, in C4_P7 at $t = 1200$ s. Nevertheless, we found no effect of sample preparation time on the extensional behavior for the polymer C4_P7, as will be shown below in Figure 10. Moreover, in oscillatory shear, the numerical values as well as the shape of the dynamic moduli of the elongation test sample rods of C4_P7 were essentially the same as those of the original pellets. This was true for all polymers studied. In addition, we analyzed the dynamic rheological behavior of the C2_P1 polymer for reactor powder, for pellets, and for the elongation rod samples. Again, there was no difference either in values or shape of the G' and G'' curves even at the lowest frequencies

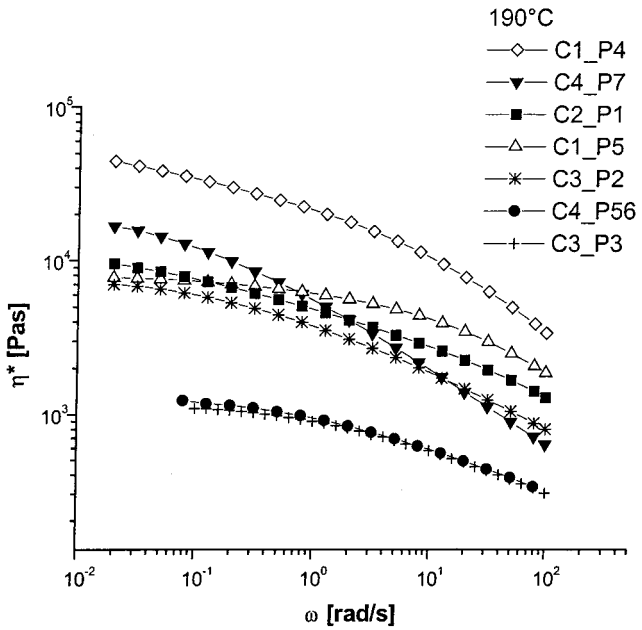

Figure 2. Complex viscosity as a function of frequency of polymers produced with catalysts **1**, **2**, **3**, and **4**. Measurements were performed at 190 °C.

analyzed. These findings confirm that the polymers were stable during the extensional sample preparation and that the behavior reported represents polymer properties produced in the polymerization reactor.

Results

Characterization by Low Shear Rheological Measurements. Table 1 lists characteristics of the polymers grouped by the catalyst used in their preparation. The zero shear viscosities η_0 given in Table 1 were obtained by creep measurements at low constant stress values. Figure 2 displays the frequency dependency of the complex viscosity for the polymers at 190 °C. It appears practical to divide the samples into three categories with respect to low shear rate viscosity and GPC-measured M_w: (1) low-molecular weight and low-viscosity polymers (C1–P6, C3–P2, and C4–P56); (2) polymers with molecular weight of approximately 100 000 g/mol and low shear rate viscosity at 190 °C of approximately 10 000 Pa•s (polymers C1–P5, C2–P55, C2–P1, C3–P2, and C4–P7); (3) polymer C1–P4 is a sample with high molecular weight and high viscosity at low shear rates. Figure 3 shows the GPC-measured molecular weight distributions of polymers with M_w values of around 100 000 g/mol: polymer C1–P5 produced with catalyst **1**, polymer C2–P1 with catalyst **2**, polymer C3–P2 with catalyst **3**, and polymer C4–P7 with catalyst **4**. Even though the MWD values of catalyst **3** and **4** polymers are fairly broad, no HMW tailing was observed, and the shape of the high MW area for polymers produced by the four catalysts was similar.

Shear rheology is extremely sensitive to presence of long-chain branching, and thus a first indication of the presence of low amounts of LCB is the zero-shear viscosity η_0 value higher than that of corresponding linear polymers of similar M_w.[5−8] This feature has also been utilized to explore the extent of metallocene LCB. Shroff and Mavridis[14] have proposed a long-chain branching index, LCBI, based on $[\eta]$ and η_0. Vega et al.[16] grouped their samples by increasing LCB utilizing the

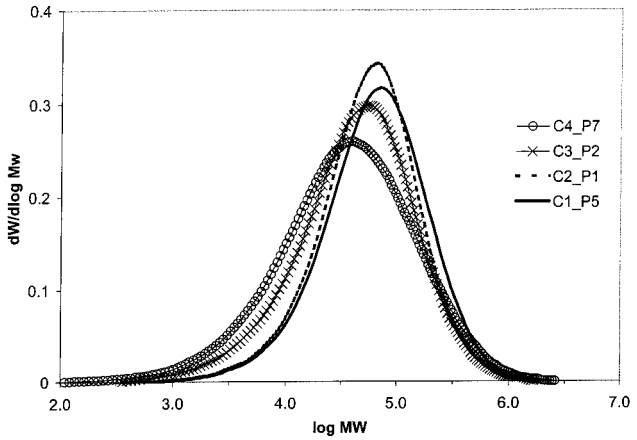

Figure 3. Molecular weight distributions measured by GPC: polymer C1–P5, polymer C2–P1, polymer C3–P2, and polymer C4–P7 produced by catalysts **1**, **2**, **3**, and **4**, respectively.

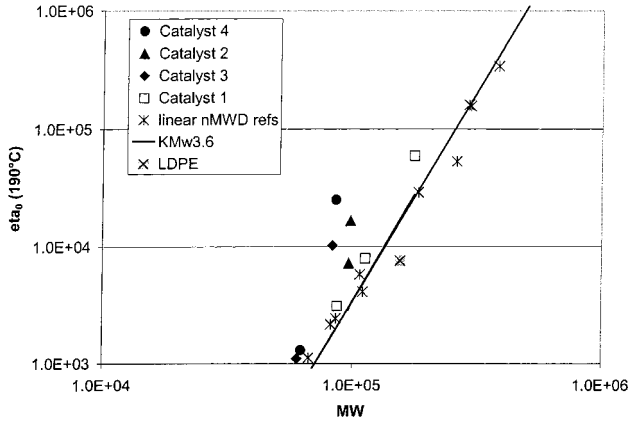

Figure 4. η_0 (190 °C) against GPC-measured M_w. The star symbols represent data of linear, narrow MWD (MWD 2.0−2.5) polymers from our earlier studies.[7,8,36] The line represents the $3.3 \times 10^{-15} M_w^{3.6}$ dependence reported by Raju et al.[35]

exponential dependence of zero shear viscosity η_0 on M_w: in LCB polymers, higher dependencies than the $\eta_0 = KM_w^{3.6}$ well-known for linear polymers[35] were obtained. Wood-Adams et al.[22] and Yan et al.[17] have evaluated the influence of LCB level on η_0 enhancement. They found that even though the η_0 increases already at LCB content of 0.2 LCB/10000C, the increase becomes more pronounced as LCB content grows. Figure 4 plots the relationship between the η_0 and GPC-measured M_w for the samples studied here. For purposes of comparison, data for linear, narrow MWD (MWD 2−2.5) ethylene homopolymers from our earlier studies[7,8,36] are included in Figure 4. The solid line in Figure 4 represents the $\eta_0 = 3.3 \times 10^{-15} M_w^{3.6}$ dependence for linear, narrow MWD HPDE polymers as reported by Raju et al.[35] The zero shear viscosity for polymers produced by catalyst **1** closely follow the 3.6 power dependence of M_w, but catalyst **2**, **3**, and **4** polymers deviate upward from the line. The deviation is largest for the catalyst **4** polymer C4–P7. In contrast, the LDPE exhibits lower η_0 than that of the corresponding linear polymers.

A method to quantitatively assess the level of long-chain branching that utilizes the extreme sensitivity of η_0 to presence of LCB was recently outlined by Janzen and Colby.[15] This method bases on the generalized phenomenological description proposed by Lusignan et al.[37] that summarizes the dependence of zero shear melt

viscosity on molecular weight, when distances between branch points that are much longer than the entanglement spacing, through formula 3

$$\eta_0 = KM_b\left[1 + \left(\frac{M_b}{M_c}\right)^{2.4}\right]\left(\frac{M_w}{M_b}\right)^{\beta} \quad (3)$$

where K is a coefficient having units of Pa·s (g/mol), M_b is an average molecular weight between branch points, M_c is the critical molecular weight for entanglements, and M_w is the molecular weight. The general behavior observed in long-chain branched polymers, namely η_0 either greater or less than the η_0 of corresponding linear polymers of similar M_w, is described by the dependence of the exponent β on M_b

$$\beta = \max\left[1, \frac{3}{2} + B\ln\left(\frac{M_b}{90M_{Kuhn}}\right)\right] \quad (4)$$

Literature values exist for K, B, M_c, and M_{Kuhn}, and thus the equations can be solved for M_b. Janzen and Colby[15] further proposed that M_b is directly related to the fraction of long-chain branch points, α, through

$$\alpha = \frac{M_0}{2}\left(\frac{1}{M_b} - \frac{1}{M_w}\right) \quad (5)$$

where M_0 is the molecular weight of the repeat unit. They reported excellent agreement between values of α and calculated stoichiometric yields for polyethylenes treated with small amounts of peroxide. Bin Wadud et al.[29] very recently reported good agreement between this method and LCB content determined by GPC-LALLS for metallocene-catalyzed LLDPEs with low levels of LCB. Inspired by these results, we evaluated our samples with the method. Following Bin Wadud et al.,[29] we used values for the constants in eqs 3−5 given in the paper by Janzen and Colby:[15] $K = 5.22 \times 10^{-6}$ (Pa·s)/(g/mol), $B = 6.0$, $M_0 = 14.027$ g/mol, $M_c = 2100$ g/mol, and $M_{Kuhn} = 145.9$ g/mol. For M_w we used values measured by GPC uncorrected for branching effects. This may have given rise to erroneous values for the long-chain branched samples but seemed a reasonable choice since GPC−on-line viscometry failed to show reliably any difference in the branching indices g' (the ratio of the intrinsic viscosity of the studied sample to that of a linear polymer, $[\eta]_{branched}/[\eta]_{linear}$) between catalyst **1**, **2**, **3**, and **4** polymers and linear polyethylene reference samples.[38] The results for K and α from formulas 3−5 are displayed in Table 1, and they will be discussed below.

Whereas linear molecules relax by reptation, long-chain branched chains require additional relaxation processes that possess a different temperature dependence than the reptation. In ethylene polymers the presence of LCB is often manifested as increased temperature dependence of the viscoelastic properties and increased value of the activation energy for flow, E_a. Moreover, in contrast to the behavior of linear polymers, outside the shear rate-independent flow region (η_0) the E_a of LCB polyethylenes is modulus-dependent. This behavior is referred to as apparent thermorheological complexity.[23,39,40] Metallocene polyethylenes with low degrees of LCB have often been reported to exhibit elevated flow activation energy,[5−8,16−18,20] and this feature has also been suggested to follow order of increasing LCB.[6,17] However, the E_a of polymers with small amount of LCB cannot always be distinguished from the E_a of linear polymers.[14,23] Table 1 shows E_a values for polymers in this study: catalyst **1** and **2** polymers exhibit flow E_a values between 32 and 34 kJ/mol, which, in comparison to literature values,[36,40,41] are in the range typical for LLDPEs with no LCB. The values obtained for the LLDPE density polymers by catalysts **3** and **4** (37−44 kJ/mol) appear clearly elevated, however. In addition, the ethylene homopolymer C3–P2, which was polymerized with the catalyst **3**, yielded flow E_a of 39 kJ/mol, which value is markedly higher than those (around 27 kJ/mol) reported for HDPE polymers of linear structure.[23,40] We note that, as can be seen in Figure 2, frequency-independent viscosity values were not reached for all samples within the frequency range used in the oscillatory experiments. Therefore, we determined the shift factors using data of the whole frequency range. The E_a values reported may thus depend on the range of data used for the determination and are probably lower than E_a values calculated from η_0 would be. Nevertheless, the E_a determined in this way fully serves our purposes of demonstrating the presence of LCB and classifying the polymers relative to one another.

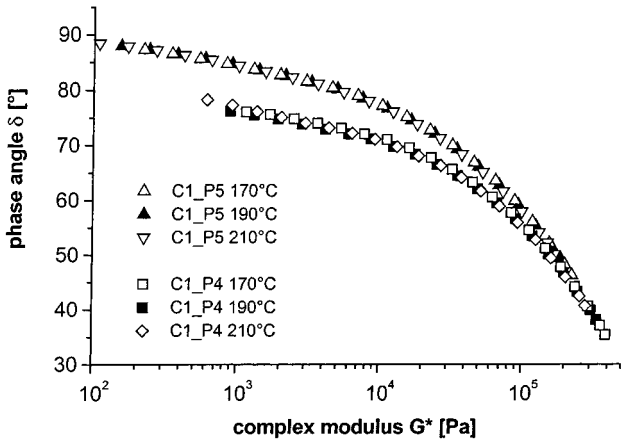

Figure 5. Phase angle as a function of complex modulus of catalyst **1** polymers C1–P4 and C1–P5. Data from 170, 190, and 210 °C.

Apparent thermorheological complexity in the linear viscoelastic behavior is conveniently detected by examining plots of either tan δ[40] or phase angle[42] vs complex modulus G^* data at different temperatures. Recently, Walter et al.[19] and Vega et al.[16] have used plots of phase angle δ vs G^* to assess also the degree of LCB, and Wood-Adams et al.[22] and Hatzikiriakos[20] have examined the effect of MWD and LCB on the phase angle δ curves. Summarizing the findings of these groups, broadening MWD and increasing LCB affect the phase angle δ vs G^* curve in a similar way: the curve is shifted to smaller phase angle values. However, apparent thermorheological complexity is seen in LCB samples only, not in linear samples of broad MWD. Figures 5−7 display phase angle δ vs complex modulus G^* data at three temperatures for the polymers with M_w around 100 000 g/mol. For polymer C1–P5 (Figure 5), the data for the three temperatures superpose very well, indicating thermorheological simplicity. For C1–P4 (Figure 5), C2–P1, (Figure 6) C3–P2, and C4–P7 (Figure 7) data from the different temperatures increasingly scatter, indicating violation of the time−temperature superposition. Shape of the phase angle curve also shows an interesting change throughout the series: in addition

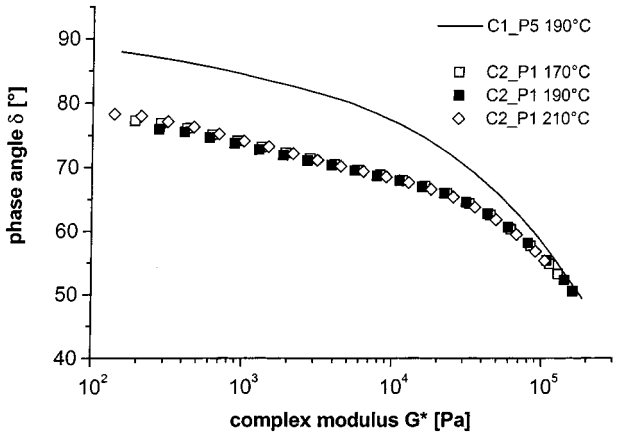

Figure 6. Phase angle as a function of complex modulus of catalyst **2** polymer C2–P1. Data from 170, 190, and 210 °C. C1–P5 data from 190 °C included as reference.

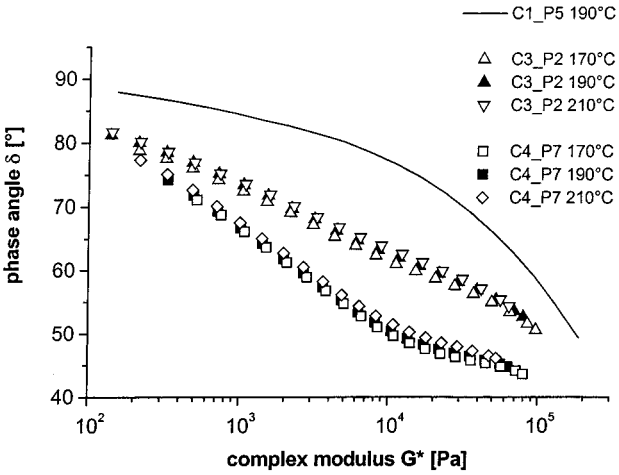

Figure 7. Phase angle as a function of complex modulus of catalyst **3** polymer C3–P2 and catalyst **4** polymer C4–P7. Data from 170, 190, and 210 °C. C1–P5 data from 190 °C included as reference.

to decreasing value of the phase angle (compared at a high value of G^*, e.g., 10 000 Pa), a plateau in the phase angle curve starts to appear. The plateau is most prominent in the phase angle curve for polymer C4–P7. Within the series, this polymer had broadest MWD, but the phase angle curve is different from that observed in broad MWD linear polyethylenes.[43] However, the shape corresponds well with the findings reported for high levels of LCB in metallocene-catalyzed, narrow MWD polymers.[16,19,20,22]

Properties in Uniaxial Elongation. In analogy to shear viscosity, the resistance against extensional flow is described as extensional (tensile) viscosity η_E. Outside the steady-state conditions, the transient extensional viscosity is dependent on both time and strain rate and is depicted as tensile stress growth coefficient η_E^+ according to formula 6

$$\eta_E^+(t, \dot{\epsilon}) = \frac{\sigma_E^+(t, \dot{\epsilon})}{\dot{\epsilon}} \tag{6}$$

where σ^+_E is the stress growth coefficient and $\dot{\epsilon}$ is the extension rate. In nonlinear, strain hardening response η_E^+ is equal to 3 times the LVE shear viscosity $\eta^+(t)$ at short times but increases sharply as the sample is further elongated. Deviation from the Trouton relation $\eta_E^+ = 3\eta^+(t)$ can be used to evaluate the degree of strain hardening through formula 7

$$\chi = \frac{\eta_E^+(t, \dot{\epsilon})}{3\eta^+(t)} \tag{7}$$

Figures 8−10 show the tensile stress growth coefficient in the constant strain rate uniaxial elongation experiments at 150 °C for selected polymers by each catalyst. The 3-fold of steady-state shear viscosity $\eta^+(t)$ from steady shear start-up measurements at 0.01 s^{-1} and 150 °C is included to indicate the linear viscoelastic behavior limit. Figure 8 shows the results for sample C1–P5: the η_E^+ curve superposes on the linear viscoelastic shear start-up curve $\eta^+(t)$ at all elongation rates, and no strain hardening is seen in the rate scale studied (1.0−0.01 s^{-1}). In contrast to C1–P5, the high-M_w polymer C1–P4 exhibits slight strain hardening behavior, the extent of which increases toward the lowest rates. Figure 9 shows the typical behavior of a LDPE in uniaxial elongation.[24] At higher extension rates, the η_E^+ rapidly increases above the linear viscoelastic limit with increasing time (and strain in the sample). At low extension rates, the transient extensional viscosity of the LDPE equals the 3-fold of the shear viscosity.

As displayed in Figures 9 and 10, polymers prepared with catalysts **2**, **3**, and **4** all exhibit strong strain hardening character at all of the elongation rates studied. Further, with the exception of C2–P55, the strain hardening behavior seems continually to increase toward the decreasing strain rates. There were differences in the polymer responses, however. The η_E^+ upturn was more severe for C2–P1 and C3–P2 than for C4–P7 and C1–P4. Flattening and roundish shape such as seen in the C4–P7 η_E^+ curves at high elongation suggest the approach of steady state in the constant strain rate tests.[44]

In the strain hardening samples, the strain hardening started approximately at Hencky strain of 1.5 at all extension rates. The samples deformed homogeneously up to the maximum Hencky strain of 3 that was attained, except for C4–P7, which approached the steady-state conditions at Hencky strain of 2.75. In the non-strain-hardening sample C1–P5, neck-in and failure started after Hencky strain 2.5. The degree of strain hardening in the constant strain rate tests was evaluated at the maximum strain, where deformation was still homogeneous. Table 2 lists the results obtained for χ from formula 7: for the non-strain-hardening sample C1–P5 the η_E^+ equaled the $3\eta^+(t)$ at all extension rates, and thus χ was 1 all the way. The LDPE showed the highest degree of strain hardening at the high elongation rates, but also polymers C2–P1, C2–P55, C3–P2, and C4–P7 exhibited considerable strain hardening at these rates. At lowest elongation rates polymer C2–P1 seemed to possess the most strain-hardening character.

In the constant tensile stress tests, steady state was achieved, and tensile viscosities η_E were obtained through

$$\eta_E = \frac{\sigma_E}{\dot{\epsilon}} \tag{8}$$

Figure 11 displays the dependence of the steady-state tensile viscosity η_E on the tensile stress. To accentuate the differences between the samples, the η_E is displayed divided by 3-fold of the steady-state shear viscosity. A curve is fitted to the data points to guide the eye.

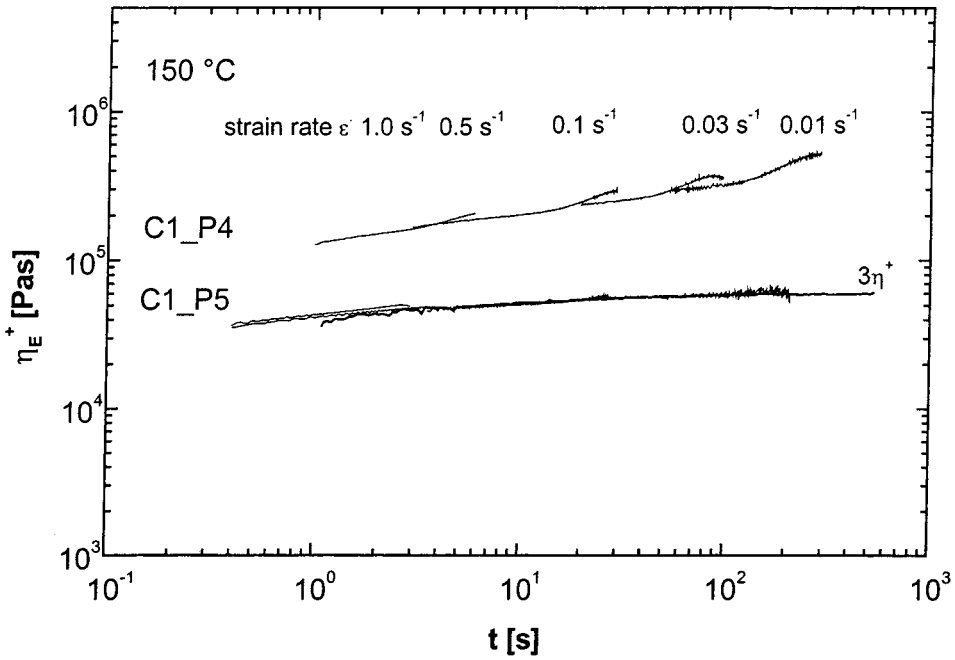

Figure 8. Time dependence of the transient tensile stress growth coefficient η_E^+ of catalyst **1** polymers C1–P4 and C1–P5 at 150 °C at various strain rates. The curve $3\eta^+$ shows the 3-fold of shear stress growth coefficient from steady shear start-up measurements at 150 °C.

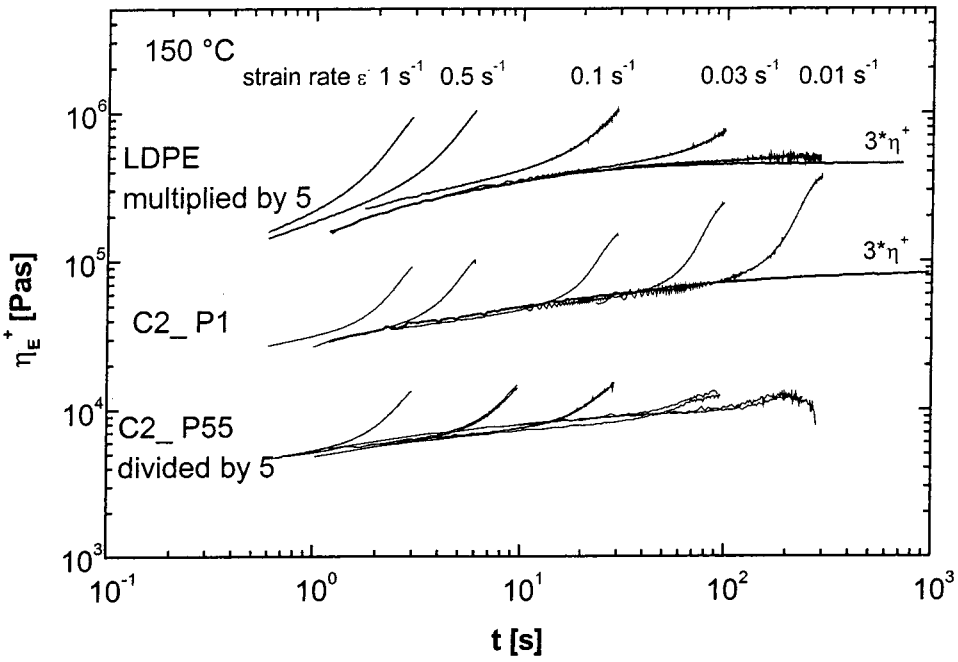

Figure 9. Time dependence of the transient tensile stress growth coefficient η_E^+ of LDPE and catalyst **2** polymers C2–P1 and C2–P55 at 150 °C at various strain rates. The curve $3\eta^+$ shows the 3-fold of shear stress growth coefficient from steady shear start-up measurements at 150 °C. For polymer C2–P55, data from two runs at strain rates 0.3, 0.1, 0.03, and 0.01 s^{-1} included to demonstrate measurement reproducibility. LDPE values have been multiplied by 5, and the C2–P55 values have been divided by 5.

Polymer C1–P5 showed stress-independent steady-state viscosity throughout the stress range measured, thus further confirming the non-strain-hardening behavior seen in the constant strain rate tests. Again, the LDPE sample showed behavior typical of LDPE polymers:[24] at low tensile stress, the η_E equaled the 3-fold of the η_0 in shear. A higher value of η_E was obtained with increase in the tensile stress. Finally, a maximum value was reached, and application of still higher tensile stress yielded extension thinning behavior: a decreased value of η_E. In contrast to LDPE, the η_E of polymer C2–P1 appeared continually to increase toward the low stress values. The steady-state extensional viscosity at the lowest stress studied exceeded the Trouton relation by a factor of 5.5, which underlines the strong strain-hardening character of this polymer. Figure 12 shows the results for C3–P2 and C4–P7 in comparison with those for C2–P1. The catalyst **3** polymer C3–P2 exhibited otherwise similar behavior to C2–P1, but the η_E increased with decreasing stress even faster than for C2–P1. In contrast, the growth of η_E for polymer C4–P7 appeared to level off at the lowest tensile stresses.

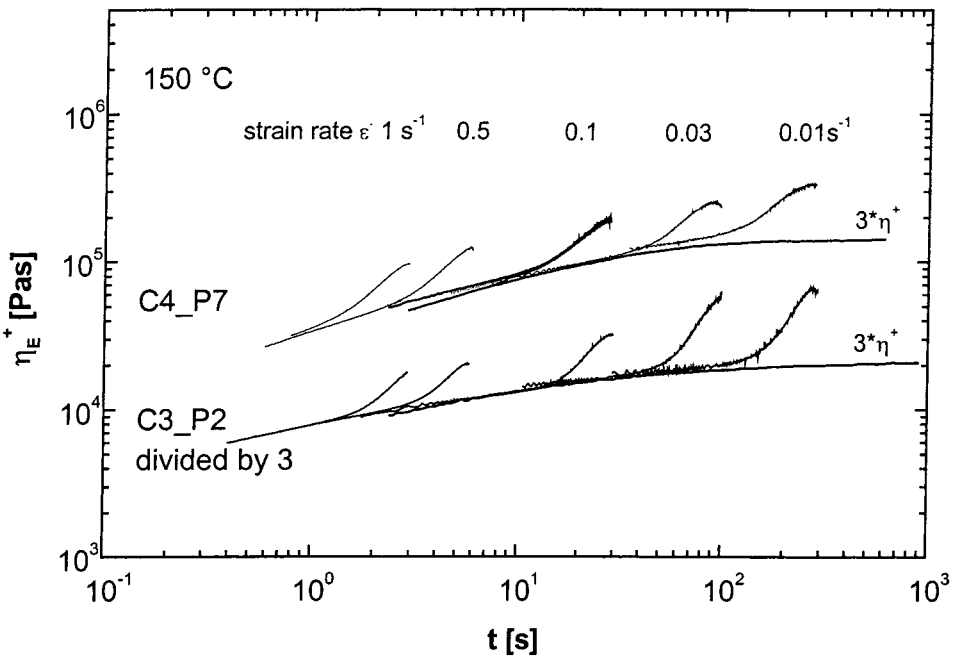

Figure 10. Time dependence of the transient tensile stress growth coefficient η_E^+ of polymer C3_P2 by catalyst **3** and catalyst **4** polymer C4_P7 at 150 °C at various strain rates. $3\eta^+$ shows the 3-fold of shear stress growth coefficient from steady shear start-up measurements at 0.01 s^{-1}, 150 °C. For C4_P7, data at strain rate 0.1 s^{-1} shows response of samples with total preparation time of 20 min and total preparation time of 30 min. C3_P2 values have been divided by 3.

Table 2. Values for the Strain-Hardening Factor, χ (Formula 7)

elongation strain rate, s^{-1}	LDPE	C1_P5	C2_P1	C3_P2	C4_P7
1.0	3.3	1.0	2.3	1.7	1.8
0.5	3.2	1.0	2.4	1.7	1.8
0.1	2.5	1.0	2.5	2.1	1.8
0.03	1.7	1.0	3.5	3.1	1.9
0.01	1.0	1.0	4.5	3.4	2.2

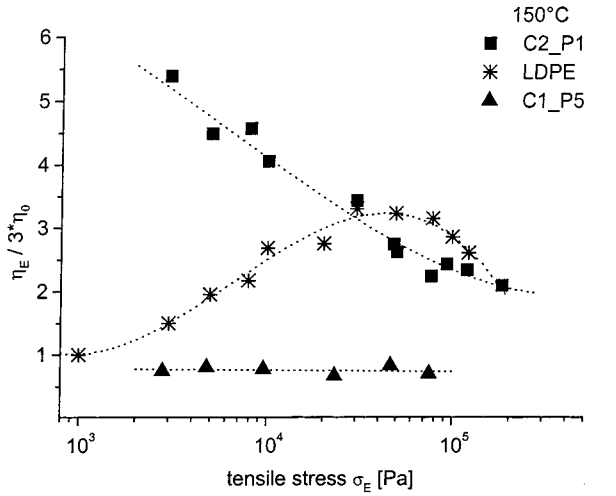

Figure 11. Steady-state elongational viscosity η_E divided by 3-fold of zero shear viscosity as a function of tensile stress for polymers C1_P5, C2_P1, and LDPE at 150 °C.

Moreover, the maximum strain-hardening value of polymer C4_P7 was only half the value obtained for C2_P1 and C3_P2.

Discussion

Relation between Molecular Structure and Uniaxial Extensional Rheological Behavior. Strain hardening in elongating flows is most often associated

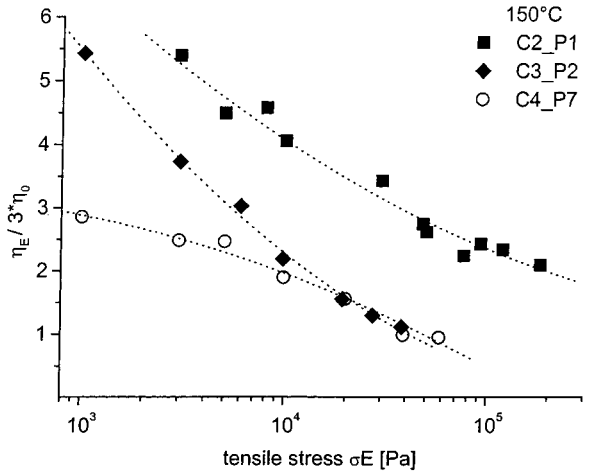

Figure 12. Steady-state elongational viscosity divided by 3-fold of zero shear viscosity as a function of tensile stress for polymers C2_P1, C3_P2, and C4_P7. Temperature 150 °C.

with long-chain branched melts, with LDPE as the most often cited example. In LDPE, increasing molecular weight shifts the extensional viscosity maximum value on the time scale toward lower times, and increasing LCB increases the value of η_E.[24] Today, it is thought that multiple-branched structures in LDPE are responsible for the nonlinear behavior; Inkson, McLeish et al.[45] have successfully modeled the nonlinear behavior of LDPE in both shear and extensional flows with idealized H-architecture. Star polymers follow the nonlinear behavior of linear melts (at least in shear rheology), whereas the strain-hardening character of the more complex H-topology has been experimentally shown with monodisperse model polymers.[46] The behavior of blends of linear and long-chain branched material of various topologies pose an interesting question. Lohse and co-workers[47] reported strain hardening at uniaxial extension rate of 1 s^{-1} in a blend of 3% of comb-structured monodisperse polybutadiene in linear mono-

disperse polybutadiene. In contrast, a blend of the linear material and 3% of 3-arm star of similar backbone and arm length as the comb did not show strain hardening.

Strain hardening has also been reported for polymers that otherwise appear to bear no long-chain branching, for example, in commercial HPDE[25,26] and LLDPE grades.[28,48] The plausible explanation for this behavior would appear to be very high molecular weight components. Gabriel et al.[49] demonstrated the presence of high-molecular weight, high-density component in ZN-catalyzed LLDPE that showed[28] strain hardening at low extension rates. Thus, it may be that the extensional measurements bear extra sensitivity to long relaxation times in general, rather than specifically for presence of long-chain branching. Consequently, knowledge of the structures present in the material, which optimally goes all the way back to the kinetics of polymerization, is required for interpretation of the results. As regards metallocene-catalyzed polyethylenes, there is strong experimental evidence for polymerization-originated long-chain branching, as was discussed in the Introduction.

Discussion of Our Findings. As regards the interdependence of the M_w, MWD, and low oscillatory shear rheology results, the polymers C1–P5 and C1–P6 produced with the unbridged catalyst **1** (*n*-BuCp_2HfCl_2/MAO) set the linear baseline for our polymer series. In addition, polymer C1–P5 exhibited non-strain-hardening behavior, further strengthening the assumption of non-long-chain branched structure for this polymer. The high-molecular weight polymer C1–P4 by catalyst **1** exhibited higher than expected low shear rate viscosity and slight strain hardening. These findings appear to demonstrate the ability of catalyst **1** to incorporate very low levels of LCB under suitable polymerization conditions.[7]

In comparison with C1–P5 and C1–P6, the polymers produced with the bridged siloxy-substituted catalysts **2**, **3**, and **4** all show signs of presence of low amounts of LCB: they deviate upward from the $\eta_0 = KM_w^{3.6}$ dependence, and they exhibit increased temperature sensitivity of the melt flow. Values for the measure of LCB, α (from formulas 3−5), for the catalyst **2**, **3**, and **4** polymers are several times higher than the values obtained for catalyst **1** polymers. It should be noted that a nonzero, though very small, value of α was obtained also for the non-strain-hardening catalyst **1** polymer C1–P5. This appears to demonstrate proportionality (relativeness) of this measure. The flow activation energy values appear to follow the order of the α values, except for the C2–P1 and C2–P3. The low-M_w polymers C3–P3 and C4–P56 yielded elevated flow E_a, but the α and the deviation from the η_0 vs M_w dependence were smaller than for the medium-molecular weight polymers C3–P2 and C4–P7. These findings indicate less LCB in the low-M_w polymers. This can be explained through the polymerization conditions; reduction in M_w was obtained by use of a larger amount of hydrogen in the polymerization, which is expected to reduce LCB formation.[7,8] Another possible explanation is the M_w of these polymers: Janzen and Colby[15] have shown that the zero shear viscosity enhancement caused by LCB depends dramatically on the M_w. To summarize, it appears from the shear rheological behavior that, at comparable M_w, polymers produced with the 1-siloxy-substituted catalysts **3** and **4** contain more long-chain branching than polymers produced with the 2-siloxy-substituted catalyst **2**. The results agree with the LCB by in situ copolymerization mechanism and with the earlier observations on the influence of catalyst structure: 1-siloxy-substituted metallocene complexes (catalysts **3** and **4**) have been found to produce polyethylene with considerable extent of vinyl endings and to copolymerize short-chain α-olefins more eagerly than 2-siloxy-substituted complexes (catalyst **2**).[8,11−13] Moreover, the copolymerization ability of 1-tri-isopropyl-siloxy-substituted catalyst (catalyst **4**) has been found to be higher than that of the 1-*tert*-butyldimethyl-siloxy-substituted catalyst (catalyst **3**).[13]

Interestingly enough, despite the only moderate changes in low shear rheology, the catalyst **2** polymer C2–P1 gave the most pronounced nonlinear behavior among the strain-hardening samples. This was true both in terms of the slope of the η_E^+ increase as well as the maximum value of η_E. It may be worthwhile to discuss the C2–P55 (Figure 9), which exhibited different strain-hardening behavior from C2–P1. It may be relevant that polymer C2–P55 was pelletized at lower temperature (190 °C) than C2–P1 (230 °C). Increase in LCB at the higher pelletization temperature of C2–P1 through reactions of the vinyl bonds is possible. However, it is not supported by the non-strain-hardening character of C1–P5, which, like the C2–P1 (and C3–P2 and C4–P7), contained measurable amounts of residual vinyl bonds and was likewise pelletized at 230 °C. Moreover, as was reported above, low oscillatory shear response of C2–P1 reactor powder, polymer pellets, and the sample rods for elongational experiments were indistinguishable, a finding which strongly speaks for no increase in LCB during either pelletization or sample preparation. The difference in elongational properties of C2–P55 and C2–P1 appears to reflect the extreme sensitivity of the uniaxial elongation technique toward fine details of the molecular structure.

Last, the shear behavior of the catalyst **4** polymer C4–P7 suggested that it contained more long-chain branching than catalyst **2** and **3** polymers. Yet the C4–P7 also exhibited lower maximum values of extensional viscosity, and unlike the others, the values approached the η_E plateau maximum value within the rate/stress scale studied. As measured by GPC, the M_w of C4–P7 was similar to that of C3–P2 and not far from that of C2–P1; thus, molecular weight offers no immediate explanation of the differences. The moderate nonlinear behavior seems to be in contradiction with the shear results: in the literature, increasing branch content has been found to enhance the nonlinear behavior and to shift the η_E^+ maximum to higher values and lower extension rates in LDPEs,[24] in polypropylene treated with cross-linking agent,[44] and in randomly branched polybutadienes.[50] As regards metallocene-catalyzed polymers with LCB, Wood-Adams et al.[21] have reported failure of uniaxial elongation data to distinguish between samples with different degree of LCB, whereas Bin Wadud et al.[29] and Chai[30] have reported more pronounced nonlinearity to indicate higher degree of LCB. None of these three studies, however, investigated the behavior at very low extension rates or with elongational creep measurements.

From the nature of the LCB formation by the copolymerization mechanism, it follows that other aspects of the LCB than the mere amount of it may be important. That the long-chain branching profoundly influences the low shear rate behavior is known from

studies with well-defined model polymers; influencing factors include length of the main chain,[15,51] branch length,[52,53]and in blends of linear and branched material also the amount of branched material.[52] Yet another influencing factor is the branching topology.[47] In the case of metallocene LCB, the copolymerization mechanism is such that each long-chain branch that is incorporated may be of the length of one whole chain. Uneven distribution of this LCB (a few multiply branched chains vs several with only one branch) would lead to species with very long relaxation times,[54,55] which, even if present in only minor amount, could be expected to significantly alter the melt flow behavior.

The behavior revealed by the uniaxial extensional measurements was only partly foreseeable in the low shear rheological results. The strain hardening behavior was expected, but in fact, the results for catalyst **2**, **3**, and **4** polymers in the LVE regime low shear studies and uniaxial elongation studies in the nonlinear range arranged the polymers in different order in terms of apparently increasing LCB. Even though both these rheological techniques are sensitive to the molecular structure, they evidently reveal different features of it. There is experimental evidence that uniaxial elongation more efficiently brings out the contribution of species with very long relaxation times, the detection of which in shear requires application of impractically low shear rates.[28,49]

We would like to propose that, in LCB metallocene-catalyzed samples, the uniaxial elongation is not so sensitive to the amount of LCB as to the LCB *distribution*, which describes whether the LCB tends to concentrate in a few multiply branched chains or to spread out in a more even manner (more chains bearing a single LCB). This being the case, the *rac*-[ethylenebis-(1-tri-isopropylsiloxy)indenyl)]$ZrCl_2$/MAO (catalyst **4**) polymers of this study would represent a more even distribution of the LCB than the polymers produced with *rac*-[ethylenebis(2-*tert*-butyldimethylsiloxy)indenyl)]$ZrCl_2$/MAO (catalyst **2**) and *rac*-[ethylenebis(1-*tert*-butyldimethylsiloxy)indenyl)]$ZrCl_2$/MAO (catalyst **3**). The catalyst plays a key role as regards the amount of LCB. Probably it also plays a role in the distribution or topology of the LCB. It is tempting to connect the more even distribution to differences in copolymerization ability. Of the catalysts employed, catalyst **4** exhibits the highest copolymerization ability toward short-chain α-olefins. It may also be that the polymerization conditions were important, but at this point we are not able to distinguish this influence. Nevertheless, in addition to the level of metallocene-originated long-chain branching, the distribution (topology) appears to be a factor. Whereas the shear rheology appears more to reflect the LCB content, the importance of the LCB distribution lies in the impact it has on the behavior in elongating flows.

Concluding Remarks

We studied shear and extensional rheological properties for polyethylenes produced with four structurally different MAO-activated metallocene complexes. The level of long-chain branching, as reflected in shear rheology, followed the copolymerization ability of the catalysts. In uniaxial elongation, the long-chain branched polymers exhibited strong strain hardening character in a wide range of extension rates (1.0−0.01 s^{-1}), and the extent of strain hardening steadily increased toward low strain rates. Interestingly, the behavior in the LVE regime shear and uniaxial elongation in the nonlinear range arranged the polymers in dissimilar order of apparently increasing LCB. To our mind, the results demonstrate the extreme sensitivity of the melt uniaxial elongation technique to differences in the molecular structure. We propose variation in the distribution (topology) of the long-chain branching due to differences in catalyst systems as a plausible explanation of the differences in the uniaxial elongation.

The literature on LCB model polymers shows that melt rheological behavior is influenced by a variety of factors, not only by the amount of long-chain branching and by the length of the main chain but also by the length and by the topology of the long-chain branching. Characterization of the long-chain branching in metallocene-catalyzed polymers is made difficult by the only low levels present. There is more to know on the influence of low levels of branching structures of different chain length on the shear rheological behavior and even more on the behavior in extensional flow. One method of this approach would be to study well-defined model polymers, and in this respect the recent advances in production of model polymers of various topologies[47] are of interest. Rheology modeling approaches, such as those presented by Janzen and Colby[15] and McLeish et al.,[46,55] which incorporate considerations of LCB architecture undoubtedly will be useful tools to investigate effects of the low levels of LCB. Finally, since the LCB is formed in the polymerization reactor, the effects of catalyst structure and polymerization conditions should not be ignored.

Acknowledgment. The financial support of the Finnish Technology Agency and Borealis Polymers Oy, enabling the visit of A. Malmberg to the University of Erlangen-Nürnberg is gratefully acknowledged. Borealis Polymers Oy is also thanked for the support provided in polymerization and polymer characterization. Special thanks to Tapio Saarinen, HUT Polymer Science Centre, for the shear creep measurements and to Dr. Markus Gahleitner, Borealis GmbH, for the valuable advise.

References and Notes

(1) Lai, S. Y.; Wilson, J. R.; Knight, G. W.; Stevens, J. C.; Chum, P.-W. S. Dow Chemical Company, U.S. Patent 5,272,236.

(2) Swogger, K. W.; Kao, C. I. Polyolefins VIII, Technol. Pap., Reg. Technol. Conf. SPE, 22.-24.2.1993, Houston, TX, 1993; p 14.

(3) Howard, P.; Maddox, P. J.; Partington, S. R. BP Chemicals Ltd., EP 0 676 421 A1.

(4) Harrison, D.; Coulter, I. M.; Wang, S.; Nistala, S.; Kuntz, B. A.; Pigeon, M.; Tian, J.; Collins, S. *J. Mol. Catal. A* **1998**, *128*, 65−77.

(5) Malmberg, A.; Kokko, E.; Lehmus, P.; Löfgren, B.; Seppälä, J. V. S. *Macromolecules* **1998**, *31*, 8448−8454.

(6) Vega, J. F.; Santamaría, A.; Muñoz-Escalona, A.; Lafuente, P. *Macromolecules* **1998**, *31*, 3639−3647.

(7) Kokko, E.; Malmberg, A.; Lehmus, P.; Löfgren, B.; Seppälä, J. V. *J. Polym. Sci., Part A: Polym. Chem.* **2000**, *38*, 376−388.

(8) Malmberg, A.; Liimatta, J.; Lehtinen, A.; Löfgren, B. *Macromolecules* **1999**, *32*, 6687−6696.

(9) Reinking, M. K.; Orf, G.; McFaddin, D. *J. Polym. Sci., Part A: Polym. Chem.* **1998**, *36*, 2889−2898.

(10) Kolodka, E.; Wang, W.-J.; Charpentier, P. A.; Zhu, S.; Hamielec, A. E. *Polymer* **2000**, *41*, 3985−3991.

(11) Kokko, E.; Lehmus, P.; Leino, R.; Luttikhedde, H. J. G.; Ekholm, P.; Näsman, J. H.; Seppälä, J. V. *Macromolecules* **2000**, *33*, 9200−9204.
(12) Lehmus, P.; Kokko, E.; Härkki, O.; Leino, R.; Luttikhedde, H. J. G.; Näsman, J. H.; Seppälä, J. V. *Macromolecules* **1999**, *32*, 3547−3552.
(13) Härkki, O.; Lehmus, P.; Leino, R.; Luttikhedde, H. J. G.; Näsman, J. H.; Seppälä, J. V. *Macromol. Chem. Phys.* **1999**, *200*, 1561−1565.
(14) Shroff, R. N.; Mavridis, H. *Macromolecules* **1999**, *32*, 8454−8464.
(15) Janzen, J.; Colby, R. H. *J. Mol. Struct.* **1999**, *485*−*486*, 569−584.
(16) Vega, J. F.; Fernández, M.; Santamaría, A.; Muñoz-Escalona, A.; Lafuente, P. *Macromol. Chem. Phys.* **1999**, *200*, 2257−2268.
(17) Yan, D.; Wang, W.-J.; Zhu, S. *Polymer* **1999**, *40*, 1737−1744.
(18) Gabriel, C.; Münstedt, H. *Rheol. Acta* **1999**, *38*, 393−403.
(19) Walter, P.; Trinkle, S.; Suhm., J.; Mäder, D.; Friedrich, C.; Mühlhaupt, R. *Macromol. Chem. Phys.* **2000**, *201*, 604−612.
(20) Hatzikiriakos, S. G. *Polym. Eng. Sci.* **2000**, *40*, 2279−2287.
(21) Wood-Adams, P. M.; Dealy, J. M. *Macromolecules* **2000**, *33*, 7481−7488.
(22) Wood-Adams, P. M.; Dealy, J. M.; deGroot, A. W.; Redwine, O. D. *Macromolecules* **2000**, *33*, 7489−7499.
(23) Wasserman, S. H.; Graessley, W. W. *Polym. Eng. Sci.* **1996**, *36*, 852−861.
(24) Münstedt, H.; Laun, H. M. *Rheol. Acta* **1981**, *20*, 211.
(25) Laun. H. M.; Schuch, H. *J. Rheol.* **1989**, *33*, 119−175.
(26) Langouche, F.; Debbaut, B. *Rheol. Acta* **1999**, *38*, 48−64.
(27) Kurzbeck, S.; Oster, F.; Münstedt, H.; Ngyen, T. Q.; Gensler, R. *J. Rheol.* **1999**, *43*, 359−374.
(28) Münstedt, H.; Kurzbeck, S.; Egersdörfer, L. *Rheol. Acta* **1998**, *37*, 21−29.
(29) Bin Wadud, S. E.; Baird, D. G. *J. Rheol.* **2000**, *44*, 1151−1167.
(30) Chai, C. K. Effect of molecular stucture on the extensional melt rheology of conventional and metallocene polyethylenes, Antec 2000, Orlando, FL, 7-11.5.2000.
(31) Malmberg, A.; Gabriel, C.; Steffl, T.; Löfgren, B. In *Proceedings of the XIIIth International Congress on Rheology, Cambridge, UK, 20-25.8.2000*, BSR, 2000; pp 1-174−1-176.
(32) Haslam, J.; Willis, H. A.; Squirrel, D. C. M. In *Identification and Analysis of Plastics*, 2nd ed.; Iliffe Books: London, 1972.
(33) Foster, G. N.; Wasserman, S. H.; Yacka, D. J. *Angew. Macromol. Chem.* **1997**, *252*, 11−32.
(34) La Mantia, F. P.; Città, V.; Valenza, A.; Roccasalvo, S. *Polym. Degrad. Stab.* **1989**, *23*, 109−119.
(35) Raju, V. R.; Smith, G. G.; Marin, G.; Knox, J. R.; Graessley, W. W. *J. Polym. Sci.* **1979**, *17*, 1183−1193.
(36) Starck, P.; Malmberg, A.; Löfgren, B. *J. Appl. Polym. Sci.* **2002**, *83*, 1140−1156.
(37) (a) Lusignan, C. P.; Mourey, T. H.; Wilson, J. C.; Colby, R. *Phys. Rev. E* **1995**, *52*, 6271−6280. (b) Lusignan, C. P. PhD Thesis, University of Rochester, 1996. (c) Lusignan, C. P.; Mourey, T. H.; Wilson, J. C.; Colby, R. *Phys. Rev. E* **1999**, *60*, 5657−5669.
(38) This may be due to artifacts such as column sensitivity or distortion of the high-M_w response in GPC−on-line viscometry analysis. On the other hand, as regards very low levels of LCB, the g' is expected to be experimentally indistinguishable from that of linear polymers.[14,15]
(39) Graessley, W. W. *Macromolecules* **1982**, *15*, 1164−1167.
(40) Mavridis, H.; Shroff, R. *Polym. Eng. Sci.* **1992**, *32*, 1778−1791.
(41) Kalyon, D. M.; Yu, D. W.; Moy, F. H. *Polym. Eng. Sci.* **1988**, *28*, 1542−1550.
(42) Van Gurp, M.; Palmen, J. *Rheol. Bull.* **1998**, *67*, 5−8.
(43) Saarinen, T.; Malmberg, A.; Löfgren, B., manuscript under preparation.
(44) Hingmann, R.; Marczinke, B. *J. Rheol.* **1994**, *38*, 573−587 point out that sometimes behavior like this is seen at the start of sample break. The steady-state viscosities η_E of C4_P7 determined by the constant stress tests corresponded closely to the η_E^+ values at high elongation, thus confirming the approach to steady-state in constant strain rate tests of C4_P7.
(45) Inkson, N. J.; McLeish, T. C. B.; Harlen, O. G.; Groves, D. J. *J. Rheol.* **1999**, *43*, 873−898.
(46) McLeish, T. C. B.; Milner, S. T. *Adv. Polym. Sci.* **1999**, *143*, 195−256.
(47) Lohse, D. J.; Xenidou, M.; Schulz, D. N.; Milner, S. T.; Fetters, L. J.; Wright, P. J.; Hadjichristidis, N.; Pitsikalis, M.; Poulos, Y.; Avgeropoulos, A.; Sioula, S.; Paraskeva, S.; Velis, G.; Mendelson, R. A.; García-Franco, C. A.; Lyon, M. K.; Sun, T.; Ruff, C. J. *Polym. Mater. Sci. Eng.* **2000**, *82*, 123−124.
(48) Micic, P.; Bhattacharya, S. N. *Polym. Eng. Sci.* **2000**, *40*, 1571−1580.
(49) Gabriel, C.; Kaschta, J.; Münstedt, H. *Rheol. Acta* **1998**, *37*, 7−20.
(50) Kasehagen, L. J.; Macosko, C. W. *J. Rheol.* **1998**, *42*, 1303−1327.
(51) Roovers, J. *Macromolecules* **1984**, *17*, 1196−1200.
(52) Graessley, W. W.; Raju, V. R. *J. Polym. Sci., Polym. Symp.* **1984**, *71*, 77−93.
(53) Gell, C. B.; Graessley, W. W.; Efstratiadis, V.; Pitsikalis, M.; Hadjichristidis, N. *J. Polym. Sci., Part B: Polym. Phys.* **1997**, *35*, 1943−1954.
(54) Beigzadeh, D.; Soares, J. B. P.; Duever, T. A.; Hamielec, A. E. *Polym. React. Eng.* **1999**, *7*, 195−205.
(55) Read, T. J.; McLeish, T. C. B. *Macromolecules* **2001**, *34*, 1928−1945.

MA010753L